

## Rheology of Long-Chain Branched Polypropylene Copolymers

Fabio Zulli,<sup>1</sup> Laura Andreozzi,<sup>1</sup> Elisa Passaglia,<sup>2</sup> Sylvain Augier,<sup>3</sup> Marco Giordano<sup>1</sup>

<sup>1</sup>Department of Physics 'Enrico Fermi', University of Pisa, and IPCF-CNR, largo Bruno Pontecorvo 3, 56127 Pisa, Italy

<sup>2</sup>ICCOM-CNR UOS Pisa, Area della Ricerca, via Moruzzi 1, 56124 Pisa, Italy

<sup>3</sup>Department of Chemistry and Industrial Chemistry, University of Pisa, 56124 Pisa, Italy

Correspondence to: L. Andreozzi (E-mail: laura.andreozzi@df.unipi.it)

**ABSTRACT:** In this work, we provide more insight into the rheological properties of functionalized polypropylene copolymers with modified architectures, which originate long-chain branching. The evaluation of the average distance between branches and the fraction of long-chain branch points has been carried out quantitatively, by numerical fitting of experimental data according to a literature model, and the viscoelastic response of the samples has been analyzed in terms of a Carreau-Yasuda-like model and Cole–Cole plots. These analyses allowed us to discriminate the viscoelastic behavior of the samples on the basis of their feed composition. Moreover, we were able to highlight direct correlations between viscosity, long-chain branching level, distance between branching points and functionalization degrees of PP polymers. © 2012 Wiley Periodicals, Inc. *J. Appl. Polym. Sci.* 000: 000–000, 2012

**KEYWORDS:** rheology; polypropylene; long-chain branching; viscosity; shear-thinning; functionalization

Received 12 March 2012; accepted 17 May 2012; published online

DOI: 10.1002/app.38076

### INTRODUCTION

Polypropylene (PP) is widely used in industrial applications because of its desirable and advantageous physical properties (high stiffness, resistance to corrosive chemicals, and low relative density). Therefore, it is apparent that modulation of the rheological properties of the melt is a main task<sup>1–10</sup> not only to obtain desired mechanical properties of the final products but also to optimize the processing conditions of PP. Indeed, melt processing and shaping of PP resins is usually obtained via extrusion and/or molding techniques, where flow conditions play important roles.

A possible way to vary the mechanical response of the material<sup>11</sup> is obtained by modifications of PP with radical mediated reactions aimed to graft functionalities and/or to change molar mass and molar-mass distribution. However, the functionalization process generally incurs drawbacks<sup>12–15</sup> such as the decreasing of molar mass; therefore, several studies have been published in recent years dealing with reagents suitable to hinder the degradation reaction through the formation of macro-radicals less liable to fragmentation.<sup>16–26</sup>

In previous works,<sup>27–29</sup> we described a procedure that allowed the functionalization of PP by peroxide initiation in the presence of macroradical stabilizers.<sup>28,29</sup> Careful analyses<sup>28,29</sup> showed improved stability and high functionalization degrees of these polymers. Also, the presence of long-chain branching (LCB) was

evidenced by a qualitative analysis of the rheological measurements<sup>29</sup> carried out to characterize the shear response of the samples. Indeed, according to literature studies, the changes of molar mass and its distribution<sup>30</sup> and the LCB formation<sup>31,32</sup> can be suitably and quantitatively detected by studying viscous and mechanical properties of the melts.

In this article, we provide more insight into the rheological investigation of the PP samples reported in Ref. 29, and quantitatively discuss the correlations between molar mass distribution, feed conditions, functionalization degree (FD), and LCB, their effects on the linear viscoelastic response of PP polymers functionalized by 3-(2-furyl)propenoate (BFA) and/or maleic anhydride (MAH),<sup>33</sup> which are able to prevent degradation reactions.<sup>34</sup> We were able to demonstrate a direct correlation between zero-shear viscosity and FD, and to evaluate the quantitative amount of LCB by applying literature models to these PP samples. Moreover, further analyses, such as the ones based on a Carreau-Yasuda-like viscoelastic model, allowed us to discriminate the effects of different functionalizers in determining the rheological response of the investigated copolymers.

### EXPERIMENTAL

#### Materials

Grafted PP copolymers with MAH and/or BFA (employed as functionalizing monomer alone or as mixtures) were prepared by commercial PP (propylene–ethylene copolymer, PPC5660)

**Table I.** Feed Composition of Functionalization Runs, FD Data, Average Molar Masses  $M_n$  and  $M_w$ , Polydispersity, and Viscosity Values Measured at 200°C of Functionalized PP Samples

Sample	ROOR <sup>a</sup> (mol %)	MAH (mol %)	BFA (mol %)	FD <sup>b</sup>	$M_n$ (kg/mol)	$M_w$ (kg/mol)	$M_w/M_n$	$\eta_0$ (Pa s)
PP	-	-	-	-	58	260	4.5	$6.25 \times 10^2$
PPMAH2	0.014	1.71	-	0.24	47	130	2.8	$1.35 \times 10^2$
PPBFA2	0.036	-	0.20	0.09	59	223	3.8	$6.90 \times 10^2$
PPBFA3	0.036	-	0.86	0.10	50	244	4.9	$1.25 \times 10^3$
PPBFA6	0.200	-	0.40	0.25	51	396	7.7	$2.00 \times 10^4$
PPMAHBFA5	0.100	0.20	0.20	0.20	55	168	3.0	$1.70 \times 10^2$
PPMAHBFA6	0.200	0.40	0.40	0.44	47	257	5.4	$3.30 \times 10^3$
PPMAHBFA7	0.300	0.60	0.60	0.59	53	298	5.6	$1.50 \times 10^5$
PPMAHBFA8	0.400	0.80	0.80	0.81	ND <sup>c</sup>	ND <sup>c</sup>	ND <sup>c</sup>	-

<sup>a</sup>ROOR = peroxide, <sup>b</sup>Number of grafted groups (FD = FDMAH + FDBFA) per 100 monomeric units (maximum standard deviation  $\pm 0.06$ ), <sup>c</sup>Sample

PPMAHBFA8 was not totally soluble in the GPC solvent at 145°C and showed a gel content of 38 wt %.

supplied by TOTAL Petrochemicals. This copolymer has an amounts of ethylene units of 23% mol,<sup>28</sup> a melting temperature of 167.4°C and a melt flow rate of 0.6–0.7 g/min (2.16 kg at 230°C). Feed conditions, functionalization degree, average molar masses, and polydispersity of the each studied sample are given in Table I; melting and crystallization temperatures are reported in Ref. 29.

Functionalization reactions were carried out in a Brabender Plastograph Mixer (mixer chamber 50 cm<sup>3</sup>). All samples were prepared with the same procedure by melt-mixing the components at 200°C and 50 rpm. After complete fusion of the pristine copolymer, functionalizing molecule(s) and the peroxide were added to the molten bulk. The reactions were carried out for 20 min and then stopped. The recovered polymer was extracted with boiling acetone and the residue was dried until constant weight. Further details about preparation of functionalizers and functionalized PP samples were described in previous papers.<sup>28,34</sup>

### Characterization

FDs were determined by using Fourier transform infrared spectroscopy following the procedure reported in Ref. 28. The FD values in Table I take into account both the grafted functionalities and refer to the total amount of grafted monomers.

The molar-mass distributions and number- and weight-average molar masses,  $M_n$  and  $M_w$ , respectively, were determined by gel permeation chromatography<sup>29</sup> using a Waters Alliance GPCV2000 apparatus equipped with three Waters Styragel HT6E columns and one Waters Styragel HT3 column, with an average particle size of 0.010 mm. The calibration was made with narrow-distributed polystyrene standards ( $M_w$  from  $5 \times 10^2$  to  $1 \times 10^7$  g/mol). A differential refractive index and a differential viscometer were used as detectors. Polymer solutions were prepared with amounts of 2.5–3.0 mg of polymer in 4 mL of 1,2,4-trichlorobenzene containing a small amount of antioxidant (butylhydroxytoluene) to prevent any degradation and then eluted at 145°C, at a flow rate of 1 mL/min.

Thermogravimetry analyses (Mettler Toledo Star System) showed a sample weight reduction of about 20% in 1 h for

pristine neat PP copolymer at 215°C under air flow of 60 mL/min. The same study, performed under nitrogen flow, showed the substantial invariance of the mass of the samples instead. For this reason, all the rheological measurements (frequency sweeps and creep-recovery experiments) were carried out at 200°C, under hyper-pure nitrogen atmosphere. As a further check, devoted to exclude the occurrence of slight molecular changes within the materials and to validate the reliability of the rheological results, the measure of viscosity was repeated for each sample before removing it from the rheometer sensors, then it was compared with its previous measurement.

Rheological measurements were performed by using a Haake Rheostress RS150H torsional rheometer, equipped with a Haake TC501 temperature control unit and with parallel plate geometry (20 mm diameter). The gap between the plates was set in the range 0.9–2.0 mm. As a caution to the influence of past stress-history, the material in the sensor system was replaced with an untreated one after each measurement set.

Frequency sweep experiments were performed in the range 0.0065–44.2 Hz. In order to work within linear viscoelastic conditions, the value of the stress has been varied to keep the value of the strain at 0.1%, as validated by amplitude sweep experiments. The loss angle  $\delta$  and the magnitude of the complex shear-modulus  $|G^*|$  were measured.<sup>35</sup> From these, material functions such as dynamic moduli  $G'$  and  $G''$  or the complex viscosity  $\eta^*$  can be obtained.<sup>35</sup>

Creep and creep-recovery experiments have been also carried out in order to evaluate zero-shear viscosity. In simple shear creep measurements, a constant stress  $\tau$  is applied to the sample and the shear strain  $\gamma$  is registered as a function of time, so that the creep compliance  $J(t)$  is evaluated as  $J(t) = \gamma(t)/\tau$ .<sup>35</sup> In the steady state of deformation, at sufficiently long creep times, the elastic part of the creep compliance becomes negligible compared to the viscous one  $t/\eta_0$ . Therefore, the zero-shear viscosity in simple creep experiments can be determined according to  $\lim_{t \rightarrow \infty} t/J(t) = \eta_0$ .<sup>35</sup> By sudden removal of the shear stress, recovery experiments are performed, to measure the recoverable portion of shear deformation and to provide the recoverable compliance  $R(t)$ . Combined use of creep and recovery

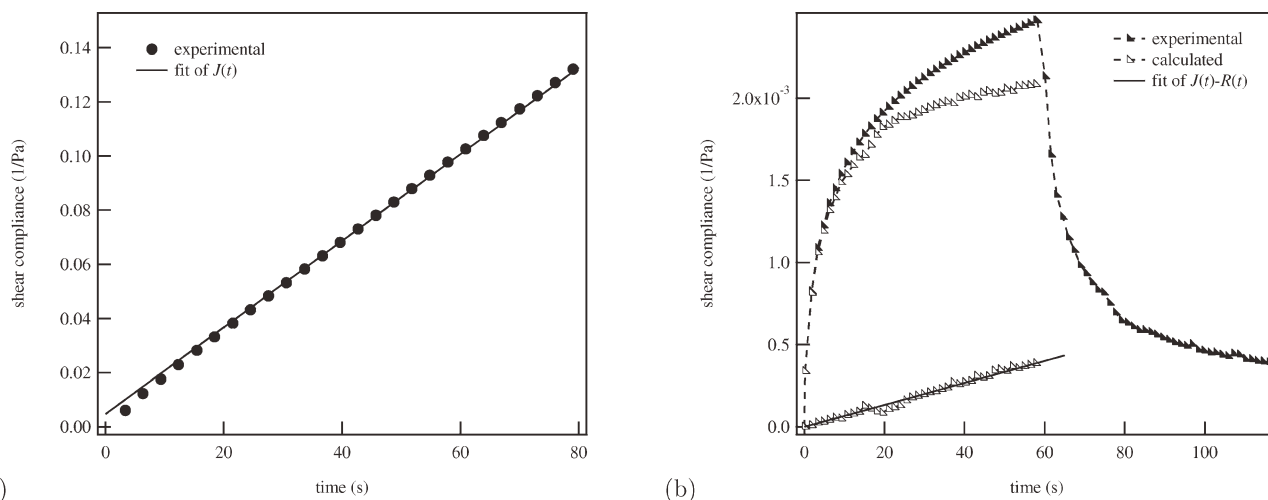


**Figure 1.** Creep experiment for PP (a) and creep-recovery for PPMAHBFA7 (b). Experimental shear compliance is shown (filled symbols) as a function of time.

experiments in the linear viscoelastic limit allows the evaluation of the viscosity of the materials, since  $J(t) = R(t) + t/\eta_0$  at all times  $t$ .<sup>36</sup> In Figure 1, examples of creep and creep-recovery experiments are shown for two of the investigated samples. The figure also reports the calculation of  $R(t)$  and  $J(t)$ . In Figure 1(a),  $J(t)$  of PP shows the asymptotic pure viscous behavior  $t/\eta$  at quite short times in the creep experiment. In Figure 1(b), the recovery of elastic component of the PPMAHBFA7 sample has to be subtracted to the creep shear compliance in order to obtain the line representing the compliance of the pure viscous component of the material  $J(t) = t/\eta$ .<sup>36</sup>

In these experiments, the occurrence of linear viscoelastic regime was tested by verifying that the compliance  $J(t)$ , obtained by a series of creep experiments for each sample, was independent of the applied stresses. Viscosity values  $\eta_0$  evaluated by creep-recovery analysis are given in Table I.

It is worth noting that pristine copolymer PPC5600 (from now on labeled as PP in this work) could exhibit a linear block character if polyethylene short blocks were randomly alternated with longer PP blocks.<sup>28</sup> In this case, the block nature of such a polymer should become apparent for those modes of the normal coordinate<sup>37</sup> approach to polymer dynamics which exhibit typical lengths comparable or smaller than block length. With regard to low-index modes (dominant in the viscous regime), they extend over a length scale such as the dynamic units of the mode turn out to be homogeneous in case of either random or block copolymers. In this study PPC5600 was characterized at 200°C, well inside the viscous regime, where the dynamic response of the polymer can be ascribed to homogeneous dynamic units. This is confirmed by the validity of time-temperature superposition principle (TTS),<sup>35,36</sup> that we have verified in the temperature range between 185–230°C. Indeed, failure of TTS is expected in the presence of inhomogeneous dynamic units, as found even for low-index modes in literature studies of diblock copolymers.<sup>38,39</sup> Therefore, the rheological response of PPC5600 behaves as that of a homopolymer above

the melt temperature. On this basis, one can expect that a 3.4 power-law dependence on molar mass  $\eta_0 \propto M_w^{3.4}$ , obeyed by linear homopolymers,<sup>37</sup> also holds for PPC5600. Such a power law was also confirmed for random copolymers,<sup>40–42</sup> and was found in ethylene/ $\alpha$ -olefin block copolymers,<sup>43</sup> whose  $\eta_0(M_w)$  were shown not to be influenced by comonomers up to hexacosene and 29 wt % of comonomer.

## RESULTS AND DISCUSSION

Figure 2 shows the frequency sweeps of the complex viscosity  $\eta^*$  of the investigated samples. The magnitude  $|\eta^*|$  is given as a function of the angular frequency in Figure 2(a), while the loss angle  $\delta$  is plotted in Figure 2(b). The loss tangent  $\tan \delta = G''/G'$  carries information about the viscous nature of a sample: in fact, a  $\delta$  angle of about 90° is found for samples with a mainly viscous behavior. In Figure 2(a), continuous lines represent best fits of the experimental curves according to a Carreau-Yasuda-like rheological model, as discussed later. On the basis of the complex-viscosity curves shown in Figure 2, the samples are grouped in three sets.<sup>29</sup>

An almost constant complex viscosity  $\eta^*$ , with the highest  $\delta$  angle values in the investigated angular frequency range, characterizes the first group of curves in Figure 2. Samples in this group show a viscous behavior due to an easy alignment and disentanglement of the chains.<sup>30</sup> In the whole investigated angular frequency range, these samples showed values of the magnitude of the complex viscosity  $|\eta^*|$  lower than those of pristine PP copolymer.

PP, and functionalized samples PPBFA2 and PPBFA3, form a second group, which shows a Newtonian plateau at low angular frequencies, and, at high angular frequencies (greater than about 6.28 rad/s), a region with decreasing complex-viscosity, hereafter referred to as shear thinning, following the nomenclature of flow-curve studies.<sup>43</sup> Even if the pristine PP copolymer has the highest  $M_w$  in this set, it shows the lowest viscosity value. This

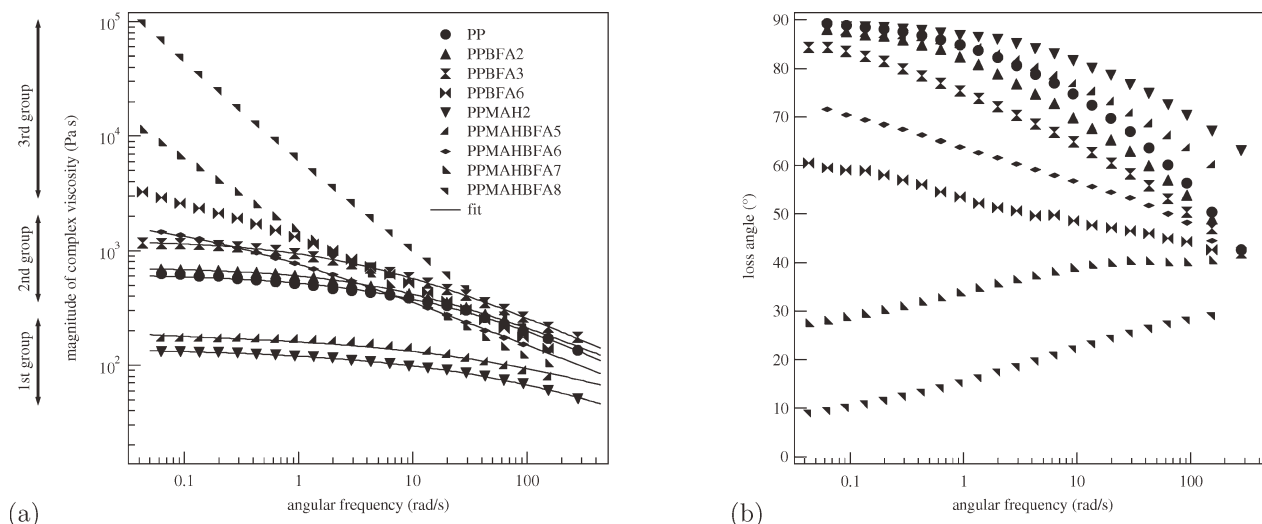


**Figure 2.** Frequency sweeps of the magnitude of complex viscosity  $|\eta^*|$  (a) and loss angle  $\delta$  (b) of functionalized PPs measured at 200°C. Same symbols refer to same samples in (a) and (b). Fits of experimental complex viscosity data according to the Carreau-Yasuda-like model of eq. (5) are also shown (a). The pertinent fitting parameters are given in Table III.

is a first indication of the presence of LCB in BFA functionalized samples: the zero-shear viscosity value is higher than that of the corresponding linear polymer of similar (or even higher) molar mass.<sup>38</sup>

It is widely reported in the literature<sup>30–32</sup> that even low amount of LCB strongly affects the viscoelastic response of polymer melts, resulting in higher Newtonian plateau, larger shear thinning, and broadened transition zone between the zero-shear viscosity and the power-law zone. PPMAHBFA6 discriminates the second and the third set, the latter exhibiting these effects, as a signature of a larger content of LCB and/or cross-linked structures.<sup>44,45</sup> Indeed for PPMAHBFA7 and PPMAHBFA8 the increasing  $\delta$  confirms the presence of such structures in the samples.

To get further insight and better discriminate the role of increasing LCB in determining zero-shear viscosity, molar mass has to be taken into account accurately. As previously discussed, it is expected that the viscosity of a linear narrow-distributed PP polymer should follow a 3.4 power-law dependence on molar mass,<sup>31</sup> according to a well-established result for high-molar-mass linear polymers and random copolymers.<sup>37,40–42,46</sup> As a consequence, linear polymers with the same  $\eta_0/M_w^{3.4}$  value would have about the same viscosity if they had the same  $M_w$ . In Figure 3,  $\eta_0/M_w^{3.4}$  data are plotted as a function of FD, in order to allow a straightforward comparison among the samples.

It is apparent that the functionalized samples used in this work show viscosities higher than the correspondent linear pristine PP copolymer with same  $M_w$ . Moreover, it can be noted that, for samples with the same set of functionalizers, the higher is the FD, the higher is the deviation from the pristine PP copolymer reference value. A power-law dependence can be detected for the set containing PP and the BFA functionalized samples. Also a general increasing trend is detectable, if one considers that the low  $M_w$  and  $\eta_0$  values for PPMAHBFA5

strongly support the idea of degradation effects for this sample: the low reagent amount did not allow the BFA to significantly prevent the beta-scission of PPMAHBFA5 polymer chains.<sup>28</sup> Degradation effects are also present in PPMAH2, where BFA was missing.

Figure 3 evidences that different viscosity values cannot be explained only in terms of the different molar-mass content. Because of the sensitivity of the rheology to chain architecture, low amounts of LCB can make viscosity values higher than

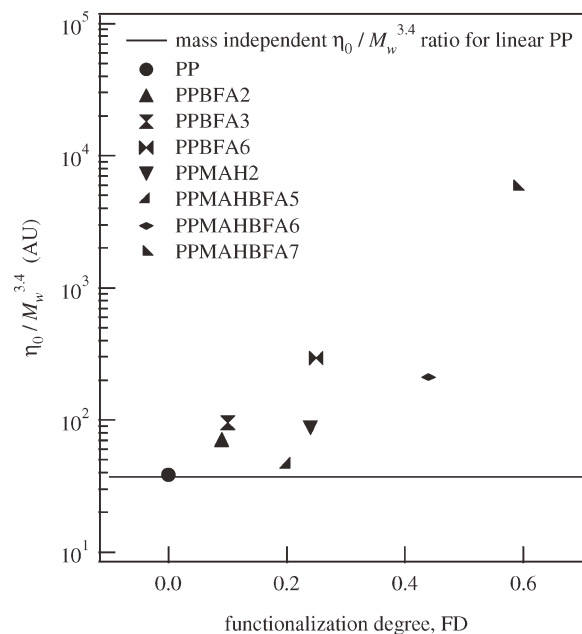


**Figure 3.** Data of the rescaled viscosity  $\eta_0/M_w^{3.4}$  plotted as a function of FD. The continuous line represents the expected mass-independent  $\eta_0/M_w^{3.4}$  ratio of linear narrow-distributed pristine PP copolymers. The  $\eta_0/M_w^{3.4}$  ratio is given in homogeneous arbitrary units.

those of the corresponding linear polymers with similar  $M_w$ , causing the deviations from the pristine PP copolymer reference value in Figure 3.

An evaluation of the amount of LCB and of the distance between branches could be obtained quantitatively, by following a model proposed by Janzen and Colby<sup>47</sup> in its turn based on the generalized phenomenological description by Lusignan and coworkers,<sup>48,49</sup> which has been widely and profitably applied to polyethylenes.<sup>30,47</sup> Accordingly, when entanglement spacing<sup>37,46</sup> is shorter than the distance between branching-points, the dependence on  $M_w$  of the zero-shear viscosity of branched polymers, is expressed by the equation:

$$\eta_0(M_w) = AM_b \left[ 1 + \left( \frac{M_b}{M_c} \right)^{2.4} \right] \left( \frac{M_w}{M_b} \right)^\beta \quad (1)$$

In eq. (1),  $M_b$  is an average molar mass between a branch point and the nearest vertex (either chain ends or other branch points) and  $M_c$  is the critical molar mass for entanglement of random branches (about the doubled value of entanglement mass of the linear homologue polymer).<sup>37,46</sup> In eq. (1), the factor  $A$  is the only parameter which depends on temperature. The dependence on  $M_b$  of the exponent  $\beta$  according to<sup>47</sup>

$$\beta = \max \left\{ 1; \frac{3}{2} + \frac{9}{8} B \ln \left( \frac{M_b}{90M_{\text{Kuhn}}} \right) \right\} \quad (2)$$

accounts for the general behavior observed in branched polymers, namely viscosities are either greater or smaller than those of their linear counterparts with same  $M_w$ .

Since  $\eta_0$  and  $M_w$  are measured quantities, if the constants  $A$ ,  $B$ ,  $M_c$  and  $M_{\text{Kuhn}}$  were known, it would be possible to solve eq. (1) for  $M_b$  when  $M_c < M_b < M_w$ . Once  $M_b$  is determined, it would also be possible to evaluate the fraction  $\alpha$  of long-chain branch points by means of<sup>30,47</sup>

$$\alpha = \frac{M_0}{2} \left( \frac{1}{M_b} - \frac{1}{M_w} \right) \quad (3)$$

where  $M_0$  is the molar mass of the repeating unit: 35 g/mol in the case of pristine copolymer, which was obtained as weighted average of 42 g/mol for PP homopolymer repeating units and 14 g/mol for PE repeating units.

The parameters  $A$ ,  $B$ ,  $M_c$  and  $M_{\text{Kuhn}}$  are available in the literature for polyethylenes,<sup>30,47</sup> but in this study similar calculation is carried out for the first time on PPs, to our knowledge. The molar masses  $M_c$  and  $M_{\text{Kuhn}}$  for PPs can be inferred from the literature<sup>50</sup>; as well as data can be retrieved regarding  $A$ .<sup>31</sup> However, information about  $B$  of PPs is not found in the literature.

Since literature does not provide the values of all the parameters, we decided to adopt the following procedure: to solve numerically eq. (1) for  $M_b$ , starting from different sets of assumed values for the other parameters  $A$ ,  $B$ , and  $M_{\text{Kuhn}}$ . Then, we repeated the procedure for all the samples and considered as correct the set of parameters that was able to provide a value of  $M_b$  from eq. (1) for all the studied samples. A confir-

mation of the goodness of the set selected in this way was also obtained by an *a posteriori* comparison with evaluations obtained by using literature data available on  $A$  and  $M_{\text{Kuhn}}$  for PP homopolymers.

To be more specific, the parameters  $A$ ,  $B$ , and  $M_{\text{Kuhn}}$  were finely varied in the ranges:  $A = 10^{-8} - 10^{-4}$  Pa s g/mol,  $B = 1.0 - 20.0$ ;  $M_{\text{Kuhn}} = 40 - 1000$  g/mol in order to determine of best set for  $A$ ,  $B$ ,  $M_c$  and  $M_{\text{Kuhn}}$ , as described. Furthermore, the critical mass  $M_c$  was fixed in order to avoid correlation between  $A$  and  $M_c$  parameters, when  $M_b$  is much greater than  $M_c$ , as drawn from eq. (1). This is because in this case the first term on the right-hand side of eq. (1) becomes negligible with respect to  $(M_b/M_c)^{2.4}$ ; consequently, the absolute value of viscosity would be determined by the factor  $A/M_c^{2.4}$ , instead of  $A$ . Likewise,  $M_c$  becomes ineffective in determining variations of  $\eta_0$  with  $M_b$ . The value of 9000 g/mol was estimated for  $M_c$  as the weighted mean of the critical molar masses<sup>40,41,50</sup> of the two species which constitute the pristine copolymer.

For each combination of the  $A$ ,  $B$ , and  $M_{\text{Kuhn}}$  parameters, a numerical routine calculated the viscosity  $\eta_0^{(\text{calc})}$  for all the  $M_w$  sample masses, varying  $M_b$  in a range between  $M_c$  and 1000 kg/mol. As soon as  $\eta_0^{(\text{calc})}$  fitted the range of the experimental viscosity value  $\eta_0 \pm 5\%$ , the corresponding  $M_b$  value was stored in a matrix, associated with the set of parameters, together with  $M_w$ ,  $\eta_0^{(\text{calc})}$ , and  $\alpha$  from eq. (3). The sets of parameters that did not fulfill this requirement for all the samples were discarded.

The further condition was imposed on the procedure: that PPMABFA7 should have been the sample with the highest  $\alpha$  (PPMABFA8 is excluded from this analysis). The distributions of the parameters fitting the above conditions turned out to have the average values:  $A = (6.5 \pm 0.3) \times 10^{-7}$  Pa s mol/g,  $B = 3.4 \pm 0.3$ ,  $M_{\text{Kuhn}} = 160 \pm 20$  g/mol. Interestingly enough,  $A$  assumes an intermediate value with the one of linear PPs and of PE<sup>31,32</sup> obtained by literature results. In fact, for well-entangled nonbranched linear polymers one expects for  $\eta_0$  the dependence  $\eta_0 = A M_w^{3.4}/M_c^{2.4}$  according to Jansen and Colby, and a law  $\eta_0 = 3.98 \times 10^{-16} M_w^{3.4}$  was found for linear PPs in Ref. 31. From the two previous laws, one obtains  $A = 3.98 \times 10^{-16} M_c^{2.4}$ , and then  $A \sim 2 \times 10^{-6}$  Pa s mol/g. Similarly, from data reported in Ref. 32, one can retrieve at 200°C the value  $A \sim 3 \times 10^{-7}$  Pa s mol/g for linear PE homopolymers. Regarding the  $B$  parameter, it has a value also found in polyethylenes.<sup>47</sup> Furthermore the value of  $M_{\text{Kuhn}}$  nicely agrees with literature results for PP and PE homopolymers. In fact, for PE homopolymers  $M_{\text{Kuhn}} = 151$  g/mol,<sup>47</sup> while Fetters et al.<sup>50</sup> reports  $0.67 \text{ \AA}^2$  mol/g as the value of the ratio of the variance  $\langle R^2 \rangle$  of the polymer end-to-end vector<sup>37</sup>  $\mathbf{R}$  to the molar mass  $M$  of the chains for PPs. Recalling that<sup>37,50</sup>

$$M_{\text{Kuhn}} = \frac{\langle R^2 \rangle M_0^2}{l_0^2 M} \quad (4)$$

where  $l_0$  is the skeletal length (about 2.6 Å for PPs) and  $M_0$  is the molar mass of the repeating unit,  $M_{\text{Kuhn}}$  can be evaluated as about 170 g/mol for PPs.



**Table II.** Distance Between Branches  $M_b$ , Fraction of Long-Chain Branch Points  $\alpha$  and Viscosity  $\eta_0^{(\text{calc})}$  Calculated for Functionalized PP Samples; Experimental  $\eta_0$  Data,  $M_w$  and  $M_b/M_w$  Are Given for Comparison

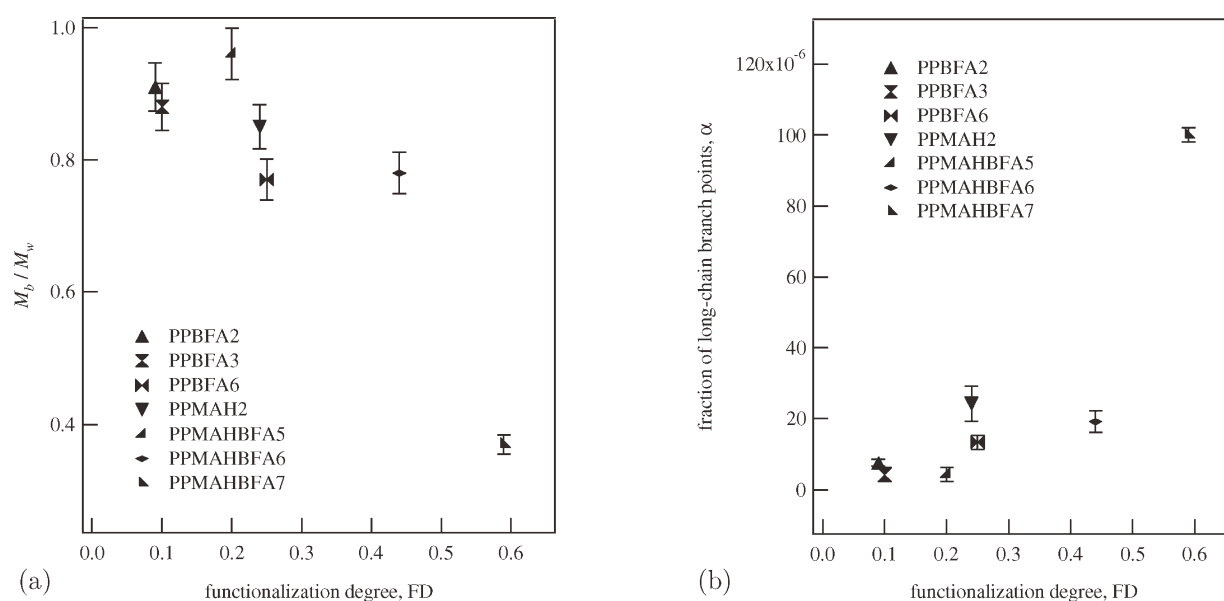
Sample	$M_w$ (kg/mol)	$M_b$ (kg/mol) <sup>a</sup>	$M_b/M_w$	$\alpha$	$\eta_0^{(\text{calc})}$ (Pa s)	$\eta_0$ (Pa s)
PPMAH2	130	110 ± 3	0.85	$(2.4 \pm 0.5) \times 10^{-5}$	$1.34 \times 10^2$	$1.35 \times 10^2$
PPBFA2	223	203 ± 2	0.91	$(0.8 \pm 0.1) \times 10^{-5}$	$7.10 \times 10^2$	$6.90 \times 10^2$
PPBFA3	244	215 ± 5	0.88	$(1.0 \pm 0.2) \times 10^{-5}$	$1.24 \times 10^3$	$1.25 \times 10^3$
PPBFA6	396	305 ± 9	0.77	$(1.3 \pm 0.2) \times 10^{-5}$	$2.02 \times 10^4$	$2.00 \times 10^4$
PPMAHBFA5	168	162 ± 2	0.96	$(0.4 \pm 0.2) \times 10^{-5}$	$1.68 \times 10^2$	$1.70 \times 10^2$
PPMAHBFA6	257	200 ± 5	0.78	$(1.9 \pm 0.3) \times 10^{-5}$	$3.39 \times 10^3$	$3.30 \times 10^3$
PPMAHBFA7	298	110 ± 9	0.37	$(1.0 \pm 0.2) \times 10^{-4}$	$1.45 \times 10^5$	$1.50 \times 10^5$

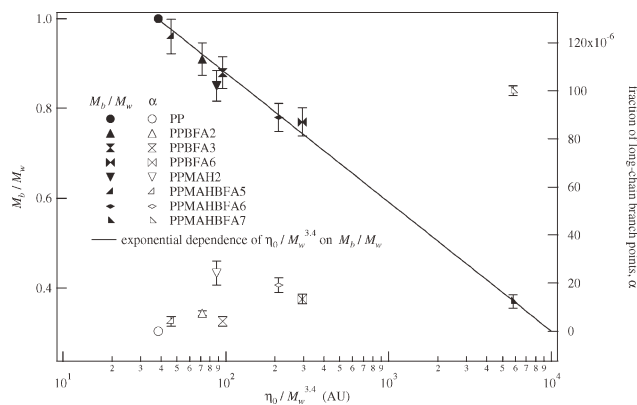
<sup>a</sup>Average  $M_b$  and its uncertainty were evaluated considering the difference between the first and last  $M_b$  values satisfying the condition  $|\eta_0^{(\text{calc})} - \eta_0|/\eta_0 < 5\%$ .

Table II gives the  $M_b$  and  $\alpha$  values calculated with the best set of parameters from the procedure described before; it also compares the calculated  $\eta_0^{(\text{calc})}$  and the experimental  $\eta_0$  viscosities (Table I). One can note the low, almost undetectable, LCB level  $\alpha$  for PPMAHBFA5, which, indeed, shows  $\eta_0$  very close to values expected for neat PP of the same  $M_w$  (Figure 3). Moreover, when the nature of the functionalizers is fixed, the ratio  $M_b/M_w$  monotonically decreases. On the other hand,  $\alpha$  monotonically increases. This behavior is magnified in Figure 4(a, b), where  $M_b/M_w$  and  $\alpha$  are shown as a function of FD, respectively. Moreover, in order to correlate displacement from reference pristine PP level of Figure 3 and LCB level,  $M_b/M_w$  and  $\alpha$  are plotted as a function of the mass-independent  $\eta_0/M_w^{3,4}$  ratio in a semilogarithmic scale in Figure 5. Direct correlation is apparent, indicating that the less is the distance between branches with regard to main-chain length, the more is the deviation of the functionalized polymer from the correspondent linear PP. An exponential law can be found describing the dependence of  $\eta_0/M_w^{3,4}$  on  $M_b/M_w$ . This is an important finding, as it clearly

shows that effects of deviations from pristine PP mass-independent  $\eta_0/M_w^{3,4}$  ratio in Figure 3 can be described quantitatively, for all the functionalized PP samples, only in terms of  $M_b/M_w$ , independently of the nature of the functionalizers.

Let us now examine in further detail the viscoelastic response of pristine PP copolymer and its functionalized copolymers. In the literature, Cole–Cole plots are used in order to underline viscous, viscoelastic, or elastic response of materials.<sup>36</sup> The Cole–Cole plots of Figure 6, show the imaginary part  $\eta''$  of complex viscosity as a function of the real part  $\eta'$  for all the copolymers of this work. Samples of the second group show a classic behavior described by an arch: the rising ramp has to be attributed to a mainly elastic response of the material, while the descending ramp is due to the viscous behavior at lower frequencies. Indeed, as degradation of the samples occurs, the PPMAH2 and PPMAHBFA5 only exhibit the descending part of the Cole–Cole arch characteristic of a viscous behavior. For data of the third group, only PPMAHBFA6 has been compared with copolymers of the previous groups; PPBFA6, PPMAHBFA7, and

**Figure 4.**  $M_b/M_w$  ratio (a) and LCB level  $\alpha$  (b) plotted as a function of FD.



**Figure 5.** Values of  $M_b/M_w$  (filled symbols) and  $\alpha$  (open symbols) plotted as a function of the mass-independent  $\eta_0/M_w^{3.4}$  ratio.

PPMAHBFA8 have been reported in the inset of Figure 6 for comparison. The three samples PPMAHBFA8 from 6 to 8 only show an ascending ramp, evidencing an ever-increasing elastic behavior up to the occurrence of a rubber-like plateau in storage modulus of PPMAHBFA8 (Figure 7) typical of LCB/cross-linked materials. From Figure 7, one can also note that the storage modulus  $G'$  for PPMAHBFA7 and PPMAHBFA8 always maintains higher values than their loss modulus  $G''$  in the investigated frequency range as expected for materials characterized by a mainly elastic response.<sup>35</sup> In Figure 7(a), dynamic modulus of the pristine PP copolymer is also shown for comparison.

For pristine PP copolymer and the other samples of the second group, it is possible to evaluate a crossing point between  $G'$  and  $G''$ . Correlation of this crossover modulus with the polydispersity index ( $M_w/M_n$ ) gives interesting information about the effects of functionalization on both molar-mass distribution and mechanical properties of the materials.<sup>51</sup> In Figure 8, crossing moduli for PPBFAs, pristine PP copolymer, and PPMAH2 are given as a function of  $M_w/M_n$ . The correlation between crossing modulus and polydispersity is confirmed. Increasing the peroxide amount leads to an increased dynamic modulus and to a

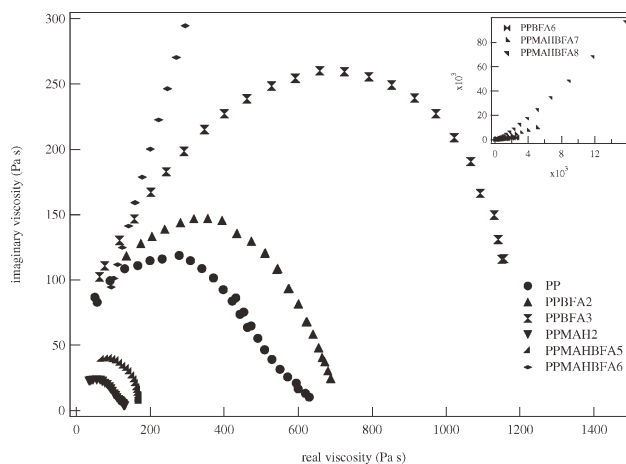


**Figure 6.** Cole-Cole plots of complex viscosity. In the inset: Cole-Cole plots of PPBFA6, PPMAHBFA7, and PPMAHBFA8.

narrower molar-mass distribution for the materials. Similar linear correlations were also reported in the literature.<sup>52,53</sup>

In the literature, rheological models have been developed in order to relate viscosity curves to empiric parameters that can be associated with the architecture of the material. Such models also allow the prediction of the rheological behavior of samples of known composition, once homologous samples have been characterized. Furthermore, by means of rheological models, it is possible to extrapolate the viscoelastic response of materials in solicitation conditions outside the instrumental range. With the aim of accomplishing further comprehension of how functionalizing runs influence the viscoelastic response of our functionalized PPs, we have fitted experimental data of  $|\eta^*(\omega)|$  with a Carreau-Yasuda-like model<sup>52</sup> (continuous lines in Figure 2)

$$|\eta^*(\omega)| = \eta'_0 [1 + (\lambda\omega)^a]^{n-1/a} \quad (5)$$

for the samples with a low-frequency Newtonian plateau (Table III). This Carreau-Yasuda-like curve shows a plateau at low

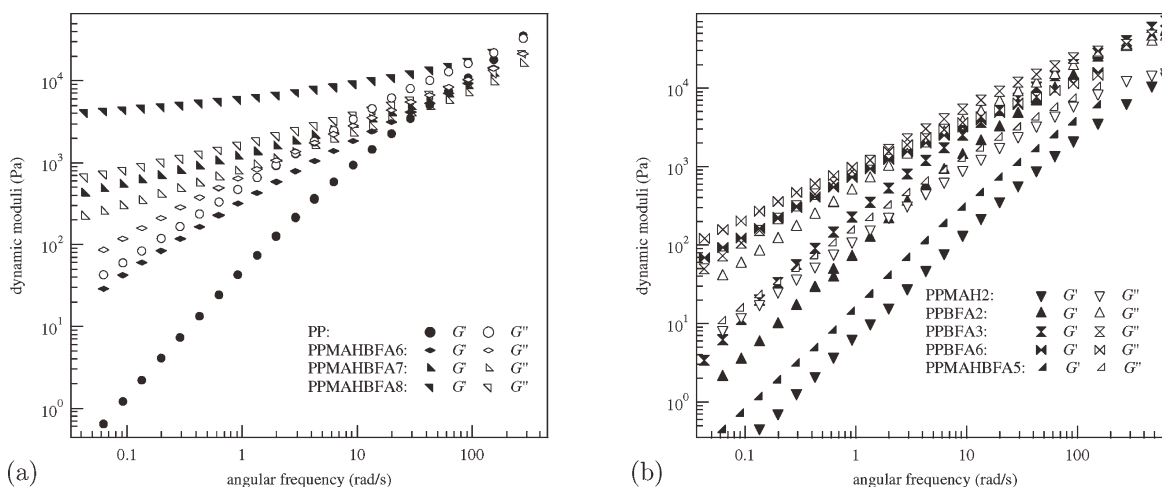


**Figure 7.** Storage  $G'$  and loss  $G''$  moduli of pristine PP copolymer, and functionalized PPMAHBFA6, PPMAHBFA7, and PPMAHBFA8 (a);  $G'$  and  $G''$  moduli of PPMAH2, PPMAHBFA5, and PPBFAs (b) as a function of the angular frequency.

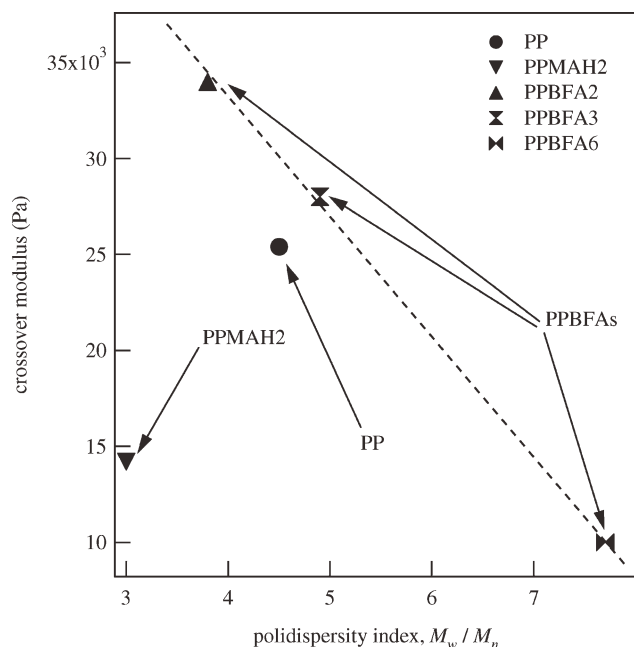


**Figure 8.** Plot of the crossover value of  $G'$  and  $G''$  as a function of the polydispersity index  $M_w/M_n$ . For some of the samples studied in this work, this crossover modulus was not detectable in the investigated frequency range. It is worth noting a linear decreasing behavior for the PPBFA series.

frequencies and a power law proportional to  $\omega^{n-1}$  at high frequencies. In eq. (5),  $\eta'_0$  represents the asymptotic value at zero frequency of the real part of complex viscosity (and hence of  $|\eta^*(\omega)|$  for mainly viscous materials),  $\lambda$  is a time carrying information about the transition from the  $\eta'_0$  plateau to the  $\omega^{n-1}$  power-law portion, while  $a$  and  $n$  are parameters describing the shape of the transition region and the slope of the rapidly decreasing portion of the curve, respectively. In the literature, expressions of eq. (5) with a yield term can also be found.<sup>52</sup> In this study this term is unnecessary to obtain good quality fits. Moreover, the authors that introduced the yield term showed<sup>52</sup> how this term becomes negligible for PP copolymers of molar mass higher than  $20 \times 10^3$  g/mol (as it is the case for our samples).

Fitting parameters of eq. (5) for the curves superimposed to experimental data of Figure 2(a) are given in Table III. It is worth noting that  $\eta'_0$  values are in agreement with zero-shear viscosity

values  $\eta_0$  found from experimental creep measurements (Table I). Moreover, we verified the validity of Cox-Merz rule,<sup>36</sup> that was assumed in other works,<sup>52,53</sup> for those samples whose steady-state viscosity curves were acquired quickly enough to avoid degradation effects (Figure 9). In fact, steady-state viscosity experiments are carried out measuring the viscosity at any selected shear-rate value until a constant value is obtained. Some of our samples degraded before reaching this condition.

Note that in Table III the fitting parameters of our samples have similar values to the ones found in literature for similar PP copolymers.<sup>52</sup> In particular, the  $n$  parameter is always lower than 1, thus indicating a shear thinning behavior. It is worth recalling that, when  $n$  tends to 1, the pure Newtonian behavior is recovered. If the nature of the functionalizers is fixed, both the parameters  $a$  and  $n$  are lowered when the molar mass is increased. This means a separation at an ever-increasing level from the Newtonian behavior with an increasing shear thinning.

Comparing the  $n$  parameter of the samples of PPBFA and PPMAHBFA series, one can note that almost the same values can be found for the samples, while PPMAH2 and pristine PP copolymer show similar  $n$  values. Therefore, BFA seems to influence the slope of the power-law of viscosity curves at high frequencies. On the other hand, both MAH and BFA functionalizers could play a role in changing the  $a$  parameter with respect to the value of pristine PP copolymer. In particular, the presence of MAH causes an  $a$  value appreciably lower, leading to a larger transition region.

From Cole–Cole plots one can deduce a characteristic relaxation time ( $\tau_{CC}$ ) of the polymers, equal to the inverse of the angular frequency corresponding to the maximum of the arches. Values for the samples of Figure 6 are given in Table III. These values can be profitably compared with the  $\lambda$  times provided by Carreau-Yasuda-like fitting (Table III): these values are substantially coincident within the experimental error. As one can note, the relaxation times increases with  $M_w$ , proportionally with viscosity when the functionalized PP series are singly considered. Moreover, the higher is the FD of the sample, the higher is the relaxation time.

## CONCLUSIONS

In this article, we discussed the rheological properties of functionalized PP copolymers, exhibiting different polymer structures, depending on the functionalization conditions.

**Table III.** Fitting Parameters of the Carreau-Yasuda-like Model of eq. (5) for Complex Viscosity and Relaxation Times Provided by Cole–Cole Plots of Figure 6

Sample	$n$	$a$	$\eta'_0$ (Pa s)	$\lambda$ (s)	$\tau_{CC}$ (s)
PP	$0.48 \pm 0.08$	$0.51 \pm 0.05$	$(6.2 \pm 0.5) \times 10^2$	$(4.3 \pm 0.3) \times 10^{-2}$	$(3.8 \pm 0.5) \times 10^{-2}$
PPMAH2	$0.49 \pm 0.08$	$0.38 \pm 0.04$	$(1.4 \pm 0.1) \times 10^2$	$(4.5 \pm 0.8) \times 10^{-3}$	$(6.3 \pm 1.5) \times 10^{-3}$
PPBFA2	$0.59 \pm 0.09$	$0.63 \pm 0.08$	$(7.1 \pm 0.4) \times 10^2$	$(1.6 \pm 0.2) \times 10^{-1}$	$(1.0 \pm 0.7) \times 10^{-1}$
PPBFA3	$0.57 \pm 0.05$	$0.62 \pm 0.09$	$(1.2 \pm 0.1) \times 10^3$	$(3.2 \pm 0.8) \times 10^{-1}$	$(2.0 \pm 0.4) \times 10^{-1}$
PPMAHBFA5	$0.59 \pm 0.08$	$0.37 \pm 0.07$	$(1.7 \pm 0.2) \times 10^2$	$(7.4 \pm 0.7) \times 10^{-3}$	$(1.5 \pm 0.8) \times 10^{-2}$
PPMAHBFA6	$0.56 \pm 0.04$	$0.32 \pm 0.04$	$(3.3 \pm 0.5) \times 10^3$	$(7.8 \pm 1.5) \times 10^0$	ND



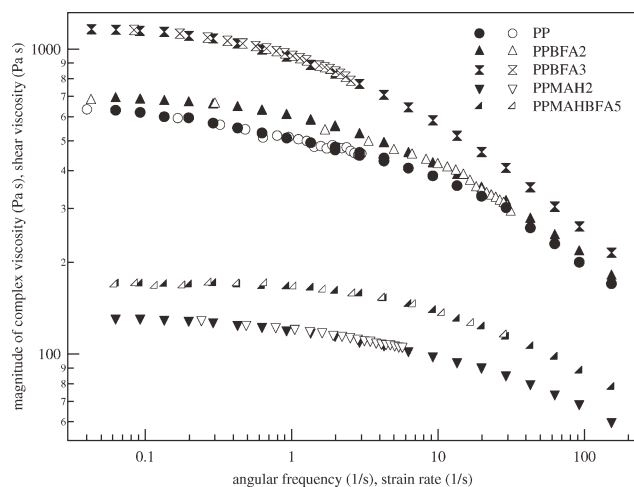


**Figure 9.** Verification of Cox-Merz rule for samples of the first and the second group. Open symbols represent  $\eta(\dot{\gamma})$  from stationary flow curves,  $|\eta^*(\omega)|$  oscillatory data are given as filled markers.

Rheological analyses highlighted these differences quantitatively. Analogies and differences among the series of samples of this work were discussed also in terms of a Carreau-Yasuda-like viscoelastic model.

Moreover, by properly taking into account molar mass contribution, we managed to discriminate the contribution of LCB in determining the viscosity of the studied functionalized PPs, observing a correlation between FD and LCB. The average distance between branches and the fraction of long-chain branch points were also quantitatively evaluated by numerical fitting of experimental data according to a literature model by Janzen and Colby.<sup>47</sup> This procedure, carried out for the first time in PPs, allowed us also to verify the consistence of the results presented here with literature data.<sup>31,50</sup> Importantly enough, this analysis strongly supports the idea of a general law, independent of the type of functionalization of the samples, describing the deviations of viscosity from that of PP nonbranched polymers only in terms of  $M_b$  and  $M_w$ .

#### ACKNOWLEDGMENTS

This work was funded by the Regione Toscana (POR OB3 Misura D4).

#### REFERENCES

1. Khellaf, S.; Khoffi, F.; Tabet, H.; Lallam, A.; Bouhelal, S.; Cagiao, M. E.; Benachour, D.; BaltaCalleja, F. J. *J. Appl. Polym. Sci.* **2012**, *124*, 3184.
2. Ardakani, F.; Jahani, Y.; Morshedian J. *J. Appl. Polym. Sci.* **2012**, *125*, 640.
3. Su, F.-H.; Yan, J.-H.; Huang, H.-X. *J. Appl. Polym. Sci.* **2011**, *119*, 1230.
4. Mandal, P. K.; Siddhanta, S. K.; Chakraborty, D. *J. Appl. Polym. Sci.* **2012**, *124*, 5279.
5. Kaseem, M.; Hamad, K.; Deri, F. *Polym. Bull.* **2012**, *68*, 1079.

6. Auhl, D.; Stadler, F. J.; Munstedt, H. *Macromolecules* **2012**, *45*, 2057.
7. Tiang, J. S.; Dealy, J. M. *Polym. Eng. Sci.* **2012**, *52*, 835.
8. Salazar, A.; Rico, A.; Rodriguez, S.; Navarro, J. M.; Rodriguez, J. S. *Polym. Eng. Sci.* **2012**, *52*, 805.
9. El Achaby, M.; Arrakhiz, F.-E.; Vaudreuil, S.; el Kacem Quiss, A.; Bousmina, M.; Fassi-Fehri, O. *Polym. Compos.* **2012**, *33*, 733.
10. Doufas, A. K.; Rice, L.; Thurston, W. J. *Rheol.* **2011**, *55*, 95.
11. Moad, G. *Prog. Polym. Sci.* **1999**, *24*, 81.
12. Gaylord, N. G.; Metha, M.; Metha, R. J. *Appl. Polym. Sci.* **1987**, *33*, 2549.
13. Chodak, I.; Lazar, M. J. *Appl. Polym. Sci.* **1986**, *32*, 5431.
14. Lazar, M.; Hrcková, L.; Borsig, E.; Marcincin, A.; Reichelt, N.; Ratzsch, M. J. *Appl. Polym. Sci.* **2000**, *78*, 886.
15. De Roover, B.; Sclavons, M.; Carlier, V.; Devaux, J.; Legras, R.; Momtaz, A. J. *Polym. Sci. Part A: Polym. Chem.* **1995**, *33*, 829.
16. Fritz, H. G.; Cai, Q.; Boelz, U. *Kunststoffe* **1993**, *86*, 439.
17. Cartier, H.; Hu, G. H. *J. Appl. Polym. Sci.* **1998**, *36*, 1053.
18. Sengupta, S. S.; Parent, J. S.; McLean, J. K. *J. Polym. Sci. Part A: Polym. Chem.* **2005**, *43*, 4882.
19. Passaglia, E.; Coiai, S.; Aglietto, M.; Ruggeri, G.; Rubertà, M.; Ciardelli, F. *Macromol. Symp.* **2003**, *198*, 147.
20. Tan, A.; Wang, W.; Hu, G. H.; Gomes, A. S. *Eur. Polym. J.* **1999**, *35*, 1979.
21. Hu, G. H.; Li, H.; Feng, L. F.; Pessan, L. A. *J. Appl. Polym. Sci.* **2003**, *88*, 1799.
22. Wang, X.; Tzoganakis, C.; Rempel, G. L. *J. Appl. Polym. Sci.* **1996**, *61*, 1395.
23. Graebing, D. *Macromolecules* **2002**, *35*, 4602.
24. Wong, B.; Baker, W. E. *Polymer* **1997**, *38*, 2781.
25. Lu, B.; Chung, T. C. *Macromolecules* **1999**, *32*, 8678.
26. Al-Malaika, S.; Kong, W. J. *Appl. Polym. Sci.* **2001**, *79*, 1401.
27. Coiai, S.; Augier, S.; Pinzino, C.; Passaglia, E. *Polym. Degrad. Stab.* **2010**, *95*, 298.
28. Augier, S.; Coiai, S.; Gragnoli, T.; Passaglia, E.; Pradel, J.-L.; Flat, J.-J. *Polymer* **2006**, *47*, 5243.
29. Augier, S.; Coiai, S.; Passaglia, E.; Ciardelli, F.; Zulli, F.; Andreozzi, L.; Giordano, M. *Polym. Int.* **2010**, *59*, 1499.
30. Malmberg, A.; Gabriel, C.; Steffl, T.; Muenstedt, H.; Loeffgren, B. *Macromolecules* **2002**, *35*, 1038.
31. Auhl, D.; Stange, J.; Muenstedt, H.; Krause, B.; Voigt, D.; Lederer, A.; Lappan, U.; Lunkwitz, K. *Macromolecules* **2004**, *37*, 9465.
32. Wood-Adams, P. M.; Dealy, J. M.; de Groot, A. W.; Redwine, O. D. *Macromolecules* **2000**, *33*, 7489.
33. Ciardelli, F.; Coiai, S.; Passaglia, E. A process of controlled radical grafting of a polyolefin. WO 2004/113399, PCT/IB2004/002098 (2004), US 2006/0148993 A1 (6 July 2006).
34. Ciardelli, F.; Augier, S.; Passaglia, E.; Coiai, S.; Pradel, J.-L.; Flat, J.-J. *Polym. Prepr.* **2006**, *47*, 600.

35. Macosko, C. W.; *Rheology: Principles, Measurements, and Applications* Wiley: New York, **1994**.
36. Morrison, F. A. *Understanding Rheology*; Oxford University Press: Oxford, **2001**.
37. Doi, M.; Edwards, S. F.; *The Theory of Polymer Dynamics* Oxford University Press: Oxford, **1986**.
38. Hirose, Y.; Urakawa, O.; Adachi, K. J. *Polym. Sci. Part B: Polym. Phys.* **2004**, *42*, 4084.
39. Park, H. E.; Dealy, J. M. *Macromolecules* **2010**, *43*, 6789.
40. Kraus, G.; Gruver, J. T. *Trans. Soc. Rheol.* **1969**, *13*, 315.
41. Ferry, J. D.; *Viscoelastic Properties of Polymers* Wiley: New York, **1980**.
42. Kim, E.; Kramer, E. J.; Garrett, P. D.; Mendelson, R. A.; Wu, W. C. *J. Mater. Sci.* **1995**, *30*, 1709.
43. Stadler, F. J.; Muenstedt, H. J. *Rheol.* **2008**, *52*, 697.
44. Sugimoto, M.; Tanaka, T.; Masubuchi, Y.; Takimoto, J.-I.; Koyama, K. J. *Appl. Polym. Sci.* **1999**, *73*, 1493.
45. Tian, J.; Yu, W.; Zhou, C. *Polymer* **2006**, *47*, 7962.
46. Andreozzi, L.; Castelvetro, V.; Faetti, M.; Giordano, M.; Zulli, F. *Macromolecules* **2006**, *39*, 1880.
47. Janzen, J.; Colby, R. H. *J. Mol. Struct.* **1999**, *485-486*, 569.
48. Lusignan, C. P.; Mourey, T. H.; Wilson, J. C.; Colby, R. H. *Phys. Rev. E* **1995**, *52*, 6271.
49. Lusignan, C. P.; Mourey, T. H.; Wilson, J. C.; Colby, R. H. *Phys. Rev. E* **1999**, *60*, 5657.
50. Fetters, L. J.; Lohse, D. J.; Graessley, W. W. *J. Polym. Sci. Part B: Polym. Phys.* **1999**, *37*, 1023.
51. Zeichner, G. R.; Patel, P. D. In *Proceedings of the Second World Congress of Chemical Engineering*, Montreal, Canada, **1981**, *6*, 333.
52. Berzin, F.; Vergnes, B.; Delamare, L. J. *Appl. Polym. Sci.* **2001**, *80*, 1243.
53. Vergnes, B.; Berzin, F. *Macromol. Symp.* **2000**, *158*, 77.